Water Research 106 (2016) 171–182

Contents lists available at ScienceDirect

Water Research

journal homepage: www.elsevier.com/locate/watres

Sub-stoichiometric titanium oxide (Ti_4O_7) as a suitable ceramic anode for electrooxidation of organic pollutants: A case study of kinetics, mineralization and toxicity assessment of amoxicillin

Soliu O. Ganiyu [a], Nihal Oturan [a], Stéphane Raffy [b], Marc Cretin [c], Roseline Esmilaire [c], Eric van Hullebusch [a], Giovanni Esposito [d], Mehmet A. Oturan [a, *]

[a] Université Paris-Est, Laboratoire Géomatériaux et Environnement (EA 4508), UPEM, 77454, Marne-la-Vallée, France
[b] SAINT-GOBAIN CREE, 550 Avenue Alphonse Jauffret, 84300, Cavaillon, France
[c] IEM (Institut Européen des Membranes), UMR 5635 (CNRS-ENSCM-UM), Université de Montpellier, Place E. Bataillon, F-34095, Montpellier, Cedex 5, France
[d] Department of Civil and Mechanical Engineering, University of Cassino and Southern Lazio, Via Di Biasio 43, 03043, Cassino, FR, Italy

ARTICLE INFO

Article history:
Received 21 July 2016
Received in revised form
25 September 2016
Accepted 27 September 2016
Available online 28 September 2016

Keywords:
Electro-oxidation
Amoxicillin
Ti_4O_7 anode
Hydroxyl radicals
Plasma deposition
Mineralization

ABSTRACT

Electrochemical degradation of aqueous solutions containing antibiotic amoxicillin (AMX) has been extensively studied in an undivided electrolytic cell using a sub-stoichiometric titanium oxide (Ti_4O_7) anode, elaborated by plasma deposition. Oxidative degradation of AMX by hydroxyl radicals was assessed as a function of applied current and was found to follow pseudo-first order kinetics. The use of carbon-felt cathode enhanced oxidation capacity of the process due to the generation of H_2O_2. Comparative studies at low current intensity using dimensional stable anode (DSA) and Pt anodes led to the lower mineralization efficiencies compared to Ti_4O_7 anode: 36 and 41% TOC removal for DSA and Pt respectively compared to 69% for Ti_4O_7 anode. Besides, the use of boron doped diamond (BDD) anode under similar operating conditions allowed reaching higher mineralization (94%) efficiency. Although Ti_4O_7 anode provides a lesser mineralization rate compared to BDD, it exhibits better performance compared to the classical anodes Pt and DSA and can constitutes an alternative to BDD anode for a cost effective electro-oxidation process. Moreover several aromatic and aliphatic oxidation reaction intermediates and inorganic end-products were identified and a plausible mineralization pathway of AMX involving these intermediates was proposed.

1. Introduction

Anodic oxidation (or electrooxidation) is one of the most popular electrochemical advanced oxidation processes (EAOPs) that able to oxidize efficiently organic pollutants present in aqueous solution. It is based on the generation of hydroxyl radicals at surface of a high O_2-overpotential anode M via water oxidation reaction (Eq. (1)) (Marselli et al., 2003; Martínez-Huitle and Ferro, 2006; Panizza and Cerisola, 2009; Sirés et al., 2014). The sorbed hydroxyl radicals (M(•OH) is non-selective highly oxidizing agent and very reactive species against organic contaminants. Therefore it is able to oxidize organic pollutants until ultimate oxidation state, i.e., mineralization (Oturan and Aaron, 2014). This process has been studied as a possible treatment technique for the remediation of wastewater with low content of various recalcitrant organic pollutants (Panizza and Cerisola, 2005; Rodrigo et al., 2014; Brillas and Martínez-Huitle, 2015; Martínez-Huitle et al., 2015).

$$M + H_2O \rightarrow M(^{\bullet}OH) + H^+ + e^- \quad (1)$$

Based on the interaction between the anode surface and sorbed hydroxyl radical, anode materials are classified into two: "non-active" anodes (e.g. BDD, PbO_2 and Ti/SnO_2) where the oxygen atom of M(•OH) is not covalently bound to the surface of the anode and "active" anodes (e.g., Pt, Ti/RuO_2, Ti/RuO_2-IrO_2 and Ti/IrO_2-Ta_2O_5) in which M(•OH) is further oxidized to form chemisorbed active oxygen with the oxygen atom covalently bound to anode surface (M = O) (Comninellis, 1994). The former (M(•OH)) usually leads to complete mineralization (electrochemical combustion) of the

* Corresponding author.
E-mail address: Mehmet.oturan@univ-paris-est.fr (M.A. Oturan).

http://dx.doi.org/10.1016/j.watres.2016.09.056
0043-1354/

substrate (Ammar et al., 2006; Ciríaco et al., 2009; Zhou et al., 2011; Fernandes et al., 2012; Oturan et al., 2012; Haidar et al., 2013; Solano et al., 2013), whereas significant mineralization of complex substrates rarely occur with the active anodes (Boye et al., 2006). BDD thin-film electrodes are the best anode material known for electrooxidation due to their high chemical stability and generation of M(•OH) in large quantities that ensures complete mineralization of organic pollutants (Murugananthan et al., 2007; Özcan et al., 2008a; Rodrigo et al., 2010; Brillas and Martínez-Huitle, 2011; Oturan et al., 2012; Diagne et al., 2014; Yu et al., 2014; García-Montoya et al., 2015). However, the high cost of BDD electrode and scarcity of suitable substrate limit its large-scale application (Panizza and Cerisola, 2009). Furthermore, relatively short service life of Ti/SnO_2-Sb based electrodes and high risk of lead contamination by chemical leaching of PbO_2 electrodes have prevent their practical applications, even though both electrodes are relatively effective for electrooxidation of organic pollutants (Chen, 2004; Lin et al., 2013).

Recently, ceramic electrodes based on sub-stoichiometric titanium oxides, particularly Ti_4O_7 has been developed and tested for potential application in electrochemical wastewater treatment (Kolbrecka and Przyluski, 1994; Chen et al., 1999). The Ti–O system belongs to Magnéli phases homologous series with the empirical formula Ti_nO_{2n-1}, ($n \geq 3$) (Andersson et al., 1957; Smith et al., 1998). Several oxides in this series exhibit high electrical conductivity at room temperature, good corrosion resistant and high chemical stability, especially $4 \leq n \leq 6$ oxides from the series, i.e., Ti_4O_7, Ti_5O_9 and Ti_6O_{11} (Chen et al., 1999; Walsh and Wills, 2010). Studies have shown that Ti_4O_7 ceramic electrode behave as non-active anode with respect to water oxidation and hydroxyl radical generation (Bejan et al., 2012; Chen et al., 1999; Geng et al., 2015). However, the M(•OH) formed at its surface appears to be less abundant when compared with BDD anode at analogous condition (Bejan et al., 2012). Although the potential of these oxides as suitable electrode in electrochemical wastewater treatment has been demonstrated in the last decade, only few studies are available in literature (Bejan et al., 2009; Chen et al., 1999; Geng et al., 2015; Zaky and Chaplin, 2014, 2013). Furthermore, relatively simple organic substrates have been investigated with little attention given to emerging micropollutants such as pharmaceutical residues.

Amoxicillin, a β-lactam antibiotic is among the most commonly detected pharmaceuticals in sewage treatment plants, effluents and surface water (Heberer, 2002; Kolpin et al., 2002; Kümmerer, 2009). It has low metabolism in both human and livestock body system; as such 80–90% is excreted and released into the environment as unmodified drug (Benito-Peña et al., 2006). Like many of other antibiotics, it is widely and unrestricted used in both human and veterinary medicine, and of great concern due to their adverse environmental impacts such as proliferation of antibiotic resistant pathogens and ecotoxicology (Costanzo et al., 2005; Pruden, 2014). Different treatment techniques have been employed for the removal of AMX from aqueous solution, including advanced oxidation processes (AOPs) such as Fenton's reagent (Elmolla and Chaudhuri, 2009; Pignatello et al., 2006; Trovó et al., 2011), ozonation (Andreozzi et al., 2005; Javier Benitez et al., 2009), heterogeneous photocatalysis (Elmolla and Chaudhuri, 2010; Klauson et al., 2010) and EAOPs using different anode materials (Panizza et al., 2014; Santos et al., 2013; Sopaj et al., 2015). Electrochemical based technologies were found to achieve much high mineralization in most cases, whereas other AOPs treatments only achieve good degradation with the formation of more stable intermediates that were mineralized at a very lower rate.

This paper investigates the potential use of the sub-stoichiometric titanium oxide (Ti_4O_7) as ceramic electrode for degradation and mineralization of AMX in aqueous medium. The effects of applied current and AMX initial concentration on the decay kinetics of AMX were systematically studied. Total Organic Carbon (TOC) decay was assessed to elucidate the mineralization of AMX. For comparison, similar studies were conducted with other known commercial anodes such as Pt, DSA and BDD. A possible reaction mechanism of the electrochemical mineralization of AMX was proposed by analyzing and quantifying the aromatic organic intermediates, short-chain carboxylic acids and released inorganic ions. Further, the evolution of solution toxicity during electrochemical treatment was examined.

2. Materials and methods

2.1. Chemicals

All chemicals used in this study were reagent grade or higher and were used as received without further purification. AMX–($C_{16}H_{19}N_3O_5S$, with >90% purity) was obtained from Sigma-Aldrich. Sodium sulfate (Na_2SO_4), sodium chloride (NaCl), potassium sulfate (K_2SO_4), sulfuric acid (H_2SO_4) and phosphoric acid (H_3PO_4) were supplied by Sigma-Aldrich, Merck, and Acros. Oxalic ($H_2C_2O_4$), oxamic ($C_2H_3NO_3$), acetic ($C_2H_4O_2$), maleic ($C_4H_4O_4$), glycoxylic ($C_2H_2O_3$) and malonic ($C_3H_4O_4$) acids were obtained from Acros, Fluka and Alfa Aesar. Bioluminescence bacteria and the activation reagent LCK 487 LUMISTOX were supplied by Hach Lange France SAS. All solutions were prepared with Milli-Q ultra-pure water (>18 MΩ at 25 °C). Organic solvents and other chemicals used were HPLC or analytic grade from Sigma-Aldrich, Fluka and Merck.

2.2. Preparation and characterization of Ti_4O_7 electrode

TiO_x particles were prepared by electro-fusion method. Briefly, a mixture of TiO_2 (ALTICHEM >98%) and coke (Coke de Brai AO151203 ALTICHEM 98%C) was fed into a Heroult-furnace and an electric arc was created between the two graphite electrodes. This electric arc was able to melt the fed mixture that was eventually poured into a graphite mold. The obtained ingot was jaw-crushed, milled and sieved to obtain powder smaller than 70 μm. The X-ray diffraction spectrum of the powder with particle size obtained shows a mixture of Ti_3O_5, Ti_4O_7, Ti_5O_9, and Ti_6O_{11} phases (Fig. 1).

The fused TiO_x particles were used to make a plasma-coating on a Ti substrate of 4 cm × 6 cm. The plasma torch (Saint-Gobain ProPlasma STD) consists of a tungsten cathode and a copper annular anode. Argon and hydrogen gas (19.6% H_2) was introduced in the space between these two electrodes. A direct current (DC) potential is applied to the electrodes; leading to an electric arc (38 kW) which ionizes both argon and hydrogen and produces a "plasma plume" with inner temperature range of 10000–15000 °C. The TiO_x particles were introduced into this plasma plume using argon as carrier gas (30 g min^{-1}; injector diameter = 1.8 mm; injection angle = +10°). They are melted and accelerated by the plasma onto the Ti substrate that has been pretreated by sand-blasting to create a rough surface. The TiOx particle size distribution (obtained from HORIBA Laser Scattering Particle Size Distribution Analyzer - PARTICA LA-950V2) is shown in Fig. 2 and indicate that 80% of the particles are in the range 20–60 μm, which is critical for plasma spraying. Melted particles impact the substrate as "splats" that are quenched at the contact of the cold titanium plate. A homogenous and continuous lamellar coating (Fig. 3) was obtained by the motion of the torch versus the substrate (linear velocity = 800 mm s^{-1}; step = 2 mm). X-ray diffraction of the prepared electrode shows that the main phase in this plasma-coating is Ti_4O_7.

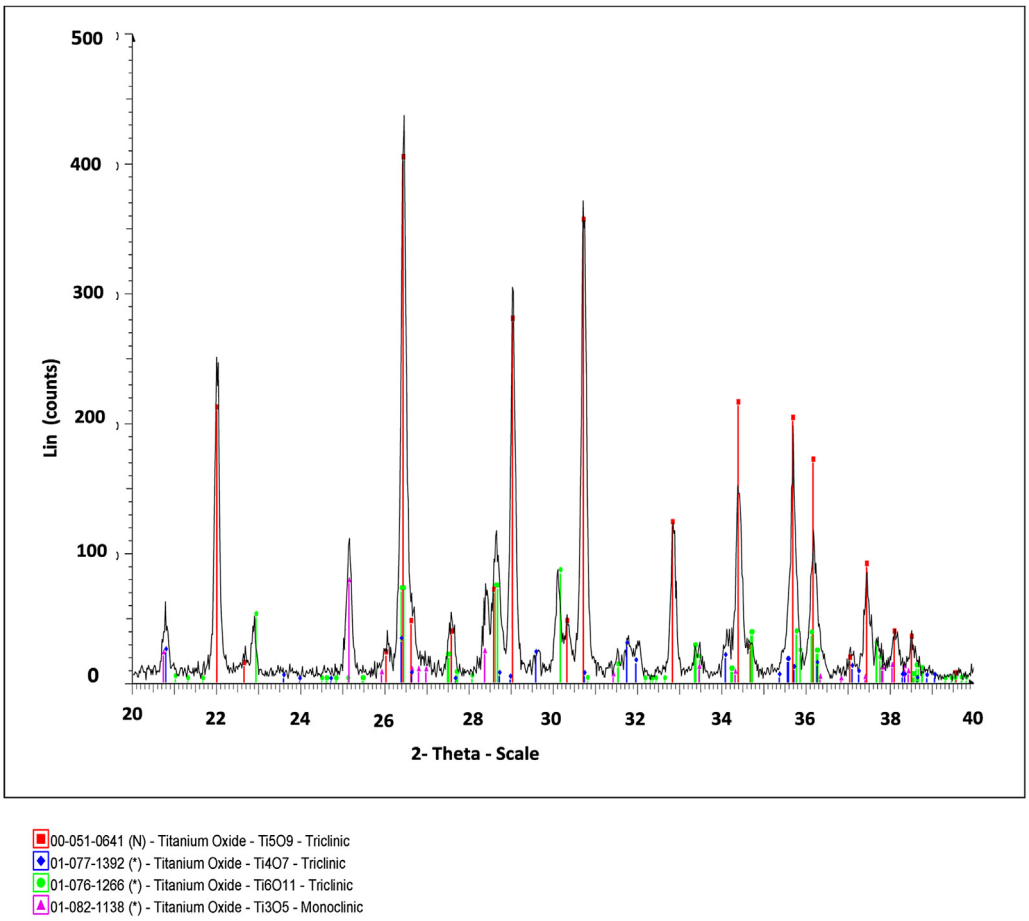

Fig. 1. X-ray diffraction pattern of the powder used in preparing Ti_4O_7 anode.

2.3. Electrolytic system

Electrolytic experiments were performed in an open, undivided and cylindrical glass cell of 6 cm diameter and 250 mL capacity with the solution vigorously stirred by a magnetic PTFE bar during treatment to enhance the mass transport towards the electrodes. A constant current was supplied with a Hameg HM8040 triple power DC supply. Four electrodes, all of 24 cm^2 area were used as anode: Ti_4O_7 (4 cm × 6 cm thin film deposited on Ti substrate, SAINT GOBAIN CREE, France), commercial pure Pt mesh, BDD (4 cm × 6 cm, CONDIAS, Germany), and commercial DSA (4 cm × 6 cm, Baoji Xinyu GuangJiDian Limited Liability Company, China). The cathode was either a tri-dimensional, large surface area carbon-felt (14 cm × 5 cm × 0.5 cm, Carbone-Lorraine, France) or stainless steel with 24 cm^2 surface area.

The anode was centered in the electrolytic cell, surrounded by the carbon-felt cathode which covers the inner wall of the cell. When using carbon-felt as cathode, compressed air was continuously bubbled into the cell through a silica frit at about 1 L min^{-1}, starting 10 min prior to electrolysis to maintain the O_2 concentration in the solution. *In-situ* H_2O_2 generation was attained by $2e^-$ reduction of dissolved oxygen at the cathode (Brillas et al., 2010). To examine the influence of applied current (10–120 mA) on AMX degradation and mineralization, 230 mL aqueous solutions of 0.1 mM AMX (19.6 mg L^{-1} TOC) containing 0.05 M Na_2SO_4 as supporting electrolyte were used to conduct the electrochemical experiments at natural pH (~5.7) of the solution. Besides, similar experiments were conducted under analogous conditions to investigate the effect of initial AMX concentrations (0.05–0.2 mM) on the degradation kinetics at applied current of 120 mA. The contribution of H_2O_2 to the degradation and mineralization of AMX was examined by substituting carbon-felt with stainless steel as cathode. All trials were conducted at room temperature (23 ± 2 °C) in duplicate.

2.4. Instruments and analytical procedures

The mineralization of treated solutions was analyzed in terms of TOC abatement, which was measured on a Shimadzu VSCH TOC analyzer according to the thermal catalytic oxidation principle. Reproducible TOC values with ±2% accuracy were found using the non-purgeable organic carbon method. The percentage TOC removal was calculated according to the following equation:

$$\text{TOC removal } (\%) = \frac{\Delta(\text{TOC})_{exp}}{\text{TOC}_0} \times 100 \quad (2)$$

where $\Delta(\text{TOC})_{exp}$ is the experimental TOC decay at electrolysis time t (mg L^{-1}) and TOC_o is the corresponding initial value before electrolysis. The mineralization current efficiency (MCE in %) was calculated from the following equation (Brillas et al., 2010):

$$\text{MCE } (100\%) = \frac{n\, FV_s\Delta(\text{TOC})_{exp}}{4.32 \times 10^7 mIt} \times 100 \quad (3)$$

where F is the Faraday constant (96487 C mol^{-1}), V_s is the solution volume (L), 4.32×10^7 is a conversion factor

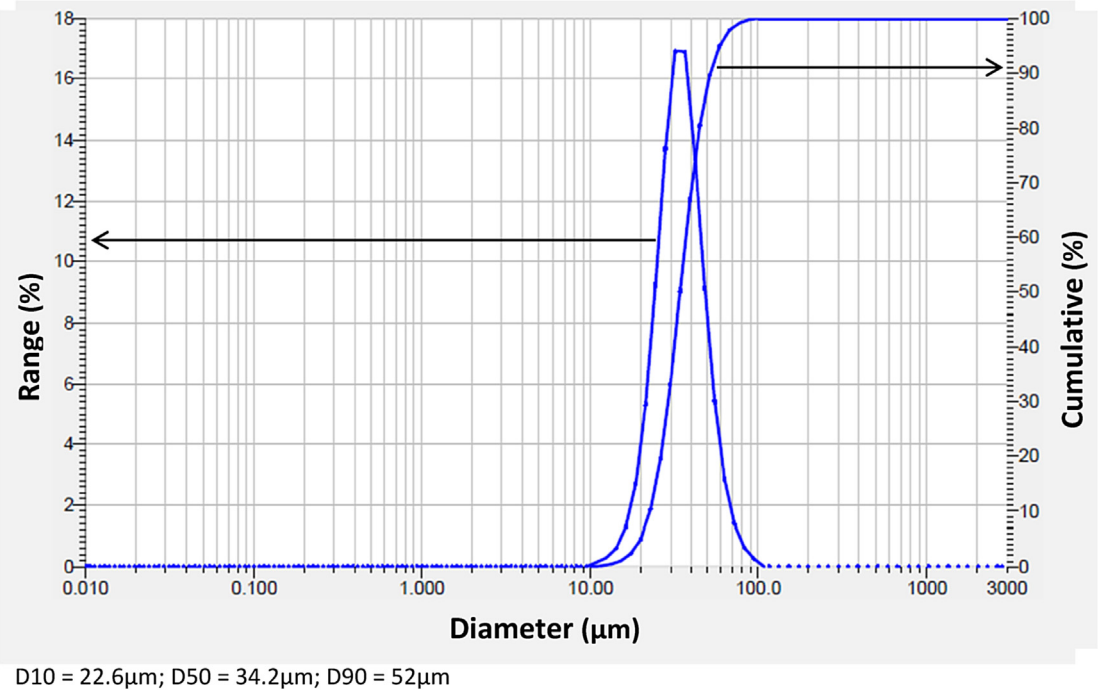

Fig. 2. TiOx particle size distribution used in preparation of Ti_4O_7.

(=3600 s h^{-1} × 12,000 mg of C mol^{-1}), *m* is the number of carbon atoms of AMX (16 C atoms) and *I* is the applied current (A) and *n* is the number of electron consumed per molecule of AMX; taken to be 70 assuming complete mineralization of AMX into CO_2, NO_3^- and SO_4^{2-}:

$$C_{16}H_{19}N_3O_3S + 42H_2O \rightarrow 16CO_2 + 3NO_3^- + SO_4^{2-} + 103H^+ + 98e^- \quad (4)$$

The concentration decay of AMX during electrolysis was analyzed by injecting 20 μL sample to the reversed-phase high performance liquid chromatography (HPLC) set-up, (Model L-7455 Lachrom, Merk Hitachi, Japan) equipped with a L-7100 pump and fitted with a Purospher RP-18, 5 μm, 25 cm × 4.6 mm (i.d.) analytical column at 40 °C with the detection performed on L-7455 photodiode array detector at a selected wavelength of 232 nm. The AMX concentration was determined periodically using an isocratic solvent elution of methanol/water (pH ~ 3 by H_3PO_4) 10:90 (v/v) as a mobile phase at a flow rate of 0.4 mL min^{-1}.

Generated aliphatic carboxylic acids during treatment were identified and quantified by ion-exclusion HPLC using Merck Lachrom liquid chromatograph equipped with an L-2130 pump, fitted with a C18 Acclaim OA (organic acids), 4 mm × 25 cm (i.d.) column at 40 °C, and coupled with a L-2400 UV detector selected at wavelength of 210 nm, using 1% H_2SO_4 at 0.2 mL min^{-1} as mobile phase. The concentrations of NO_3^-, NH_4^+ and SO_4^{2-} released to the treated solutions were assessed on ion chromatography by injecting 50-μL samples into a Dionex ICS-1000 Basic Ion Chromatography set-up coupled with a Dionex DS6 conductivity detector containing a cell maintained at 35 °C through Chromeleon SE software. The NO_3^- and SO_4^{2-} content were determined with a

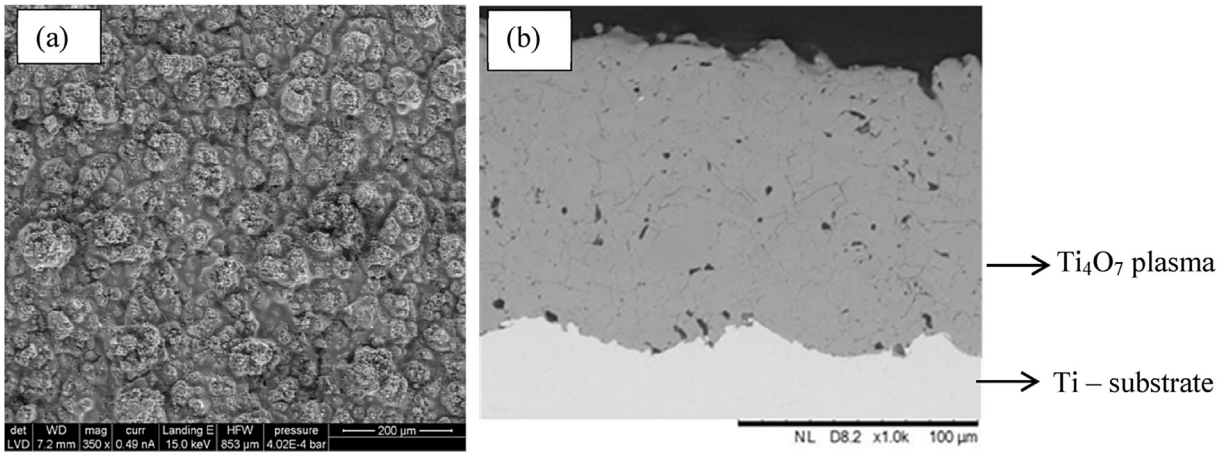

Fig. 3. SEM image of the prepared Ti_4O_7 anode (a) surface, and (b) cross-section.

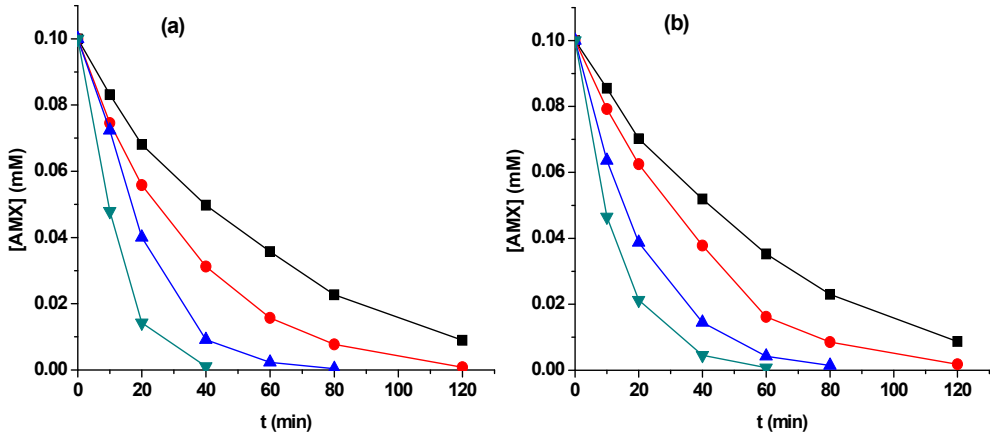

Fig. 4. Effect of applied current: (-■-) 10 mA (-●-) 30 mA, (-▲-) 60 mA and (-▼-) 120 mA on AMX concentration decay vs. electrolysis time for the electrooxidation treatment of 0.1 mM AMX in 0.05 M Na_2SO_4 using (a) Ti_4O_7 and (b) BDD anode and carbon-felt cathode.

Dionex AS4A-SC, 25 cm × 4 mm (i.d.) anion-exchange column using a mixture of 1.8 mM Na_2CO_3 and 1.7 mM $NaHCO_3$ solution at 2.0 mL min^{-1} as mobile phase. For NH_4^+ detection, a Dionex CS12A, 25 cm × 4 mm (i.d.) cation column and a mobile phase of 9 mM H_2SO_4 at 1.0 mL min^{-1} was used.

GC-MS analyses were performed using a Thermo Scientific GC-MS analyzer equipped with a TRACE 1300 gas chromatography coupled to an ISQ single quadrupole mass spectrophotometer operating in electron impact mode at 70 eV. Samples for GC-MS were obtained by solvent extraction of organic components of 10 cm^3 of electrolyzed solution with 45 cm^3 of dichloromethane (three extractions with 15 cm^3 each), followed by drying of the organic fraction over 2 g of $MgSO_4$, filtered and concentrated to a volume of 1 cm^3 with a rotary evaporator under vacuum. The samples were directly analyzed by GC-MS using a TG-5MS 0.25 μm, 30 m × 0.25 mm (i.d.), column, with a temperature ramp of 50 °C for 3 min, 10 °C min^{-1} up to 250 °C and 4 min hold time. The temperature of the injector and detector were 200 and 250 °C respectively, and helium was used as carrier gas at a flow rate of 1.5 mL min^{-1}. The mass spectra were identified by Xcalibur data library.

The evolution of toxicity of treated AMX solutions at different electrolysis times was performed by means of Microtox® method. Toxicity of the samples was evaluated based on the inhibition of the bio-luminescence of the bacteria *V. fischeri*. The pH of all the analyzed samples was adjusted to 6.5–7.5 with the aid of 0.1–0.01 mM NaOH, and the bioluminescence measurements were performed on both blank as well as electrolyzed AMX solutions after 5 and 15 min of exposure to *V. fischeri* bacteria using Microtox method.

Table 1
– Apparent rate constants ($k_{app,AMX}$) for the electrooxidation of AMX by **M(•OH)**, assuming pseudo first-order reaction.

Cell	$k_{app,\ AMX}$ (min^{-1})				
	[AMX] (mM)	10 mA	30 mA	60 mA	120 mA
DSA/CF	0.1				0.02
Pt/CF	0.1				0.05
Ti_4O_7/CF	0.05				0.12
	0.1	0.02	0.03	0.07	0.10
	0.2				0.05
Ti_4O_7/SS	0.1			0.02	0.03
BDD/CF	0.05				0.10
	0.1	0.02	0.03	0.05	0.08
	0.2				0.04
BDD/SS	0.1			0.03	0.05

3. Results and discussion

3.1. Kinetic studies of AMX degradation

The kinetics of the degradation of AMX by electrogenerated oxidants especially M(•OH) has been studied from the decay of its concentration monitored by reversed-phase HPLC. A well-defined absorption peak related to AMX was always displayed at a retention time (t_R) of 10.8 min on the chromatograms. As shown in Fig. 4a and b, the decay of AMX concentration is dependent on the applied current and much rapid degradation was observed with increasing current with both Ti_4O_7 and BDD anodes. The concentration of AMX reduced to 0.09 mM (~4.0 mg L^{-1}) in both cases when a lower current of 10 mA was applied for 120 min, whereas it was completely degraded after 120 and 80 min at 30 and 60 mA respectively. However, a slightly faster decay in AMX concentration was observed with Ti_4O_7 anode at 120 mA (Fig. 4a), with the drug disappeared after 40 min compared to 60 min observed with BDD anode (Fig. 4b). The increase in reaction rate of AMX with raising current is related to the production of more quantity of electrogenerated active oxidant (M(•OH)) from water oxidation at anode surface (Eq. (1)), which rapidly oxidize AMX molecules. Comparative studies at 120 mA with DSA and Pt anodes and carbon-felt cathode show lower degradation rate as expected with active anodes, with AMX concentration drops to ~0.04 mM (1.5 mg L^{-1}) after 120 min with DSA anode and disappeared from the solution after 80 min with Pt anode, due to smaller quantity of M(•OH) generated at their surfaces and high chemisorption of generated •OH to anode surface.

In all case, the oxidation of AMX by M(•OH) was fitted with pseudo first-order kinetic reaction assuming a quasi-stationary state for M(•OH) concentration, since it is very reactive and cannot be accumulated in the medium. This implies that a constant concentration of M(•OH) always reacts with AMX (Brillas et al., 2010; Sirés et al., 2010; Oturan and Aaron, 2014). The analysis of the plots using linear regression yielded apparent rate constant ($k_{app,AMX}$) values that are summarized in Table 1, with excellent linear correlations ($R^2 \approx 0.99$). As shown in Table 1, the $k_{app,AMX}$ values gradually increases as the current raises from 10 to 120 mA with both Ti_4O_7 and BDD anodes. It is worthy to note that $k_{app,AMX}$ values for both anodes are relatively close with slightly better values for Ti_4O_7 anode at 60 and 120 mA.

The influence of AMX concentration (0.05, 0.1 and 0.2 mM) on

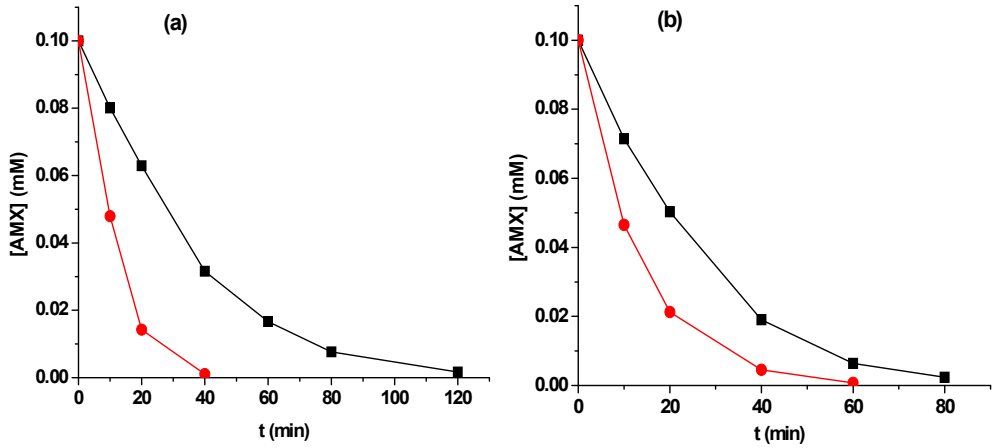

Fig. 5. Contribution of in-situ generated H_2O_2 to the decay of AMX concentration vs time with stainless steel cathode (-■-) and carbon-felt cathode (-●-) for the electrooxidation at 120 mA of 0.1 mM AMX in 0.05 M Na_2SO_4 using (a) Ti_4O_7 and (b) BDD anode.

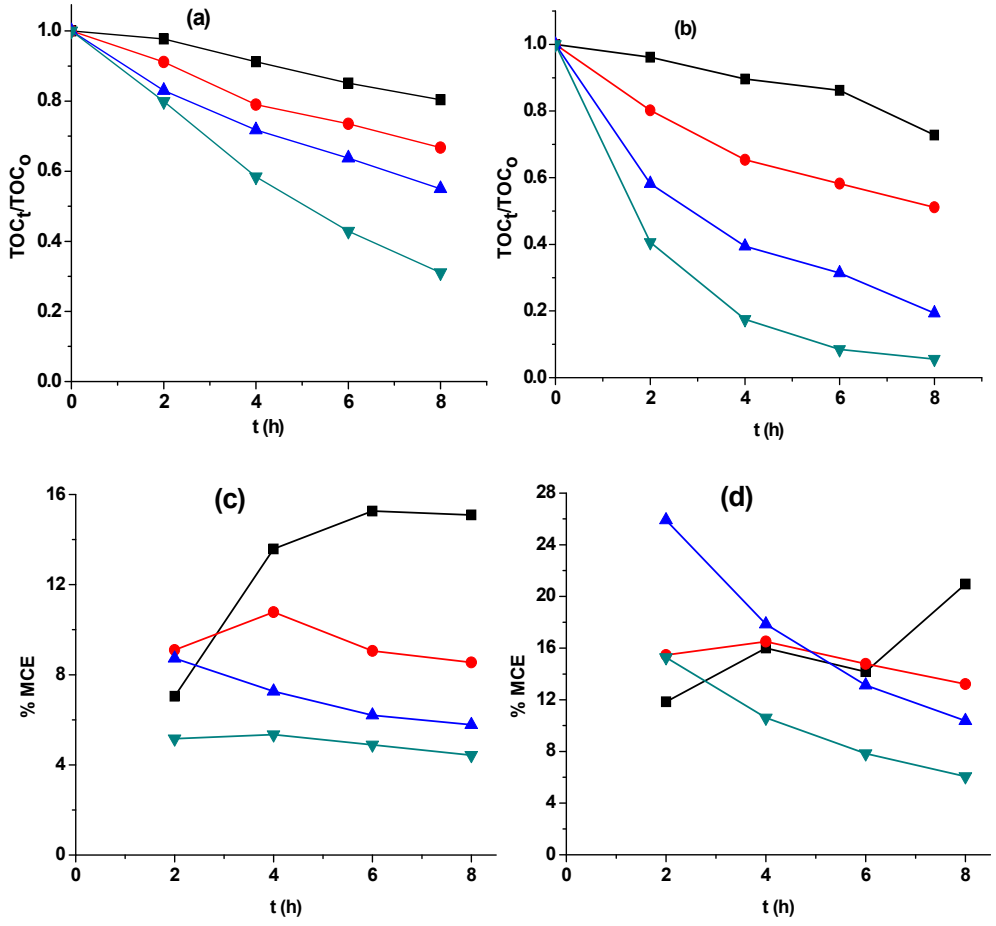

Fig. 6. Effect of applied current: (-■-) 10 mA (-●-) 30 mA, (-▲-) 60 mA and (-▼-) 120 mA on TOC removal (a, b) and mineralization current efficiency (c, d) vs. electrolysis time during the electrooxidation of 0.1 mM (19.6 mg L^{-1} initial TOC) AMX in 0.05 M Na_2SO_4 using Ti_4O_7, (a, c) and BDD (b, d) anode and carbon-felt cathode.

its degradation kinetic, studied at applied current of 120 mA with both Ti_4O_7 and BDD anodes shows that AMX was completely removed from the medium after short electrolysis times of 40, 60 and 80 min for 0.05, 0.1 and 0.2 mM concentrations, respectively, demonstrating the high potential of Ti_4O_7 anode in electro-oxidation of organics even at high concentration level. The $k_{app,AMX}$ values (Table 1) diminished with increasing of initial AMX concentrations from 0.05 to 0.2 mM with both anodes. This is logical because under analogous experimental conditions, identical concentration and nature of oxidants, especially M(•OH) are generated at the surface of anode. As such, high ratio of oxidants to AMX is expected at lower initial concentration, suggesting greater possibility of AMX oxidation that resulted into higher $k_{app,AMX}$ values. Additionally, huge quantity of intermediates by-products is

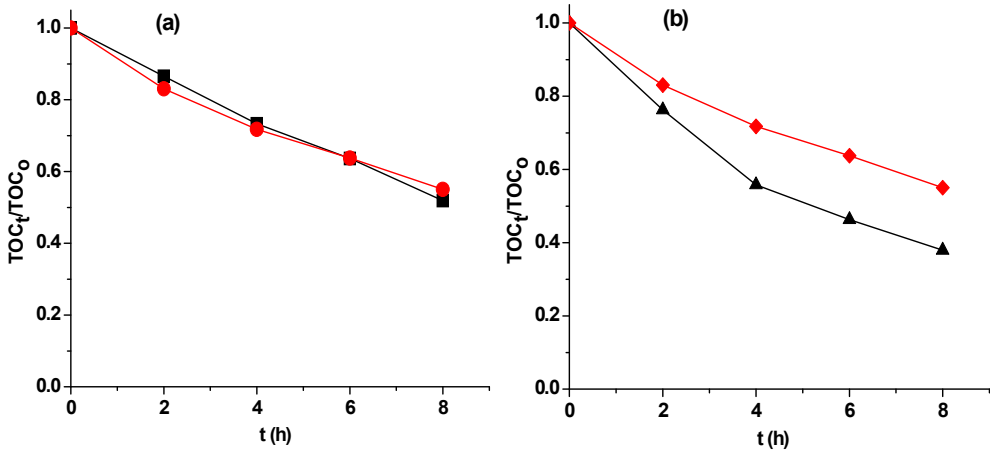

Fig. 7. – (a) Effect of in-situ generated H_2O_2 on the mineralization of 0.1 mM AMX (19.6 mg L^{-1} TOC) in 0.05 M Na_2SO_4 medium at applied current of 60 mA, (-■-) without H_2O_2 (stainless steel cathode) and (-●-) with H_2O_2 generation using Ti_4O_7 anode. (b) Stability of activity of Ti_4O_7 with usage time for mineralization of 0.1 mM AMX (19.6 mg L^{-1} TOC) in 0.05 M Na_2SO_4 medium at applied current of 60 mA: (-▲-) < 25 h, (-♦-) > 200 h of usage.

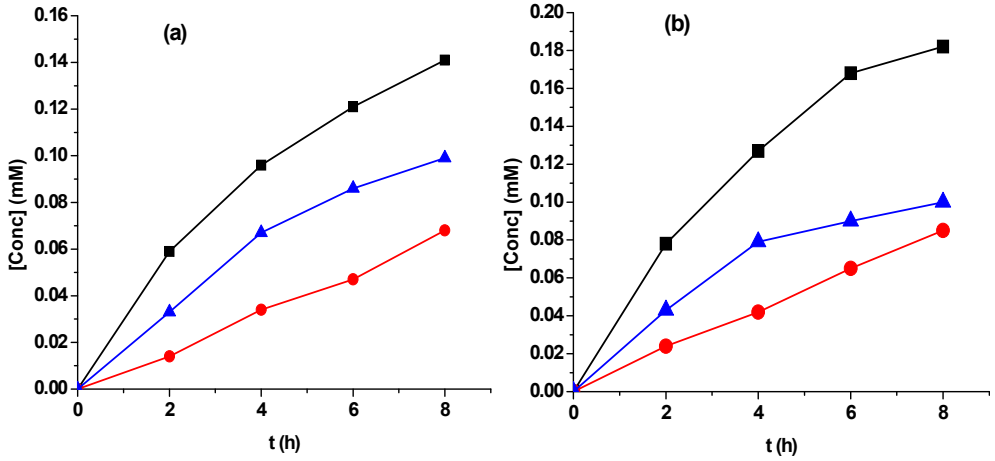

Fig. 8. Time-course of the identified inorganic ions: (-■-) NH_4^+ (-●-) NO_3^- and (-▲-) SO_4^{2-} during the electrooxidation of 0.1 mM AMX in 0.05 M K_2SO_4 (for NH_4^+) and NaCl (for SO_4^{2-}) analyses during constant current electrolysis at 120 mA using (a) Ti_4O_7 and (b) BDD anode and carbon-felt cathode.

expected to be generated at higher initial concentration, thus limiting the reaction between AMX molecules and M(•OH) since the latter is a non-selective radical and will also react with formed intermediates species.

To clarify the contribution of H_2O_2 as a weak oxidant to AMX concentration decay with both Ti_4O_7 and BDD anodes, experiments were carried out by replacing carbon-felt with stainless steel as cathode. Carbon-felt is well known for H_2O_2 generation potential, whereas stainless steel has a very limited capacity for H_2O_2 generation (Özcan et al., 2008b). Fig. 5a and b shows the contribution of H_2O_2 to the AMX degradation assessed from experiment performed at 120 mA using Ti_4O_7 and BDD anodes. It is obvious that the generated H_2O_2 contributes significantly to the decay of AMX concentration in the treated solution. The decay rate of AMX tremendously decreased when carbon-felt was replaced by stainless steel as cathode material. However, the decrease in degradation rate was more slightly pronounced with Ti_4O_7 when compared with BDD. The generated H_2O_2 contribution is either by direct oxidation as a weak oxidant or indirectly after its destructive reaction with M(•OH) to generate hydroperoxyl radical M(HO_2•) (Eq. (5)) (Brillas et al., 2010):

$$H_2O_2 + BDD(^{\bullet}OH) \rightarrow BDD(HO_2^{\bullet}) + H_2O \quad (5)$$

It must be noted that the oxidation of AMX by either of these oxidants (H_2O_2 or M(HO_2•)) mainly leads to the formation of stable intermediates with very limited mineralization as it is explained in section 3.2.

3.2. Mineralization of AMX solution

The potential of Ti_4O_7 as a suitable anode for electrochemical oxidation of AMX was assessed by studying the mineralization of 0.1 mM AMX solutions (corresponding to 19.6 mg L^{-1} initial TOC) at varying applied current from 10 to 120 mA. Fig. 6a depicts the decay of TOC vs electrolysis time at different applied current obtained for the experiments performed with Ti_4O_7 anode. An improved mineralization degree with rising in applied current and electrolysis time with final TOC removal being 20%, 33%, 45% and 69% at 10, 30, 60 and 120 mA, respectively, was obtained after 480 min of electrolysis. This behavior agrees with the generation of high quantity of M(•OH) from water oxidation (Eq. (1)), leading to quick oxidation of both AMX and its intermediates as explained in section

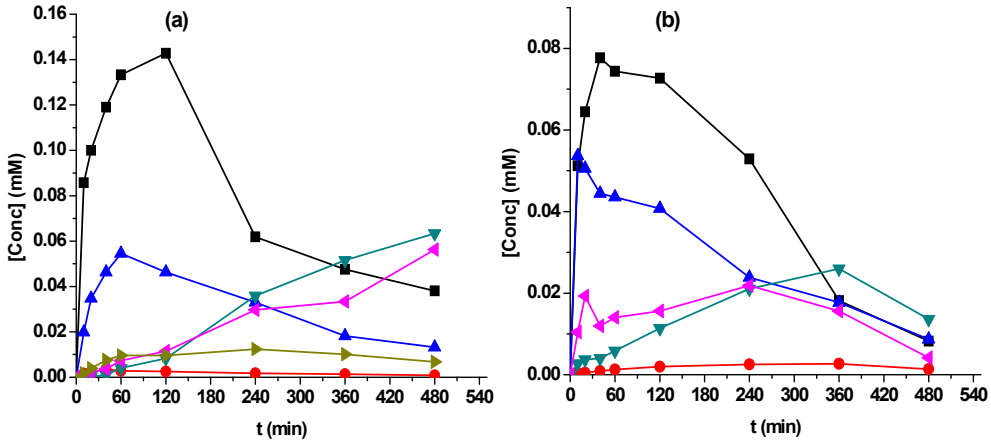

Fig. 9. Time-course of the identified short-chain carboxylic acids: (-■-) oxalic; (-●-) maleic; (-▲-) malonic (-▼-) oxamic; (-◀-) acetic; (-▶-) glyoxylic during the electrooxidation of 0.1 mM AMX in 0.05 M Na_2SO_4 solution at 120 mA using (a) Ti_4O_7 and (b) BDD and carbon-felt cathode.

3.1. Relatively low mineralization was obtained at lower applied current (10 and 30 mA) due to lower anodic potential (≤water discharge potential) which limits the generation of M(•OH) (Zaky and Chaplin, 2013). However, improved mineralization was obtained when applied current was increased from 30 to 120 mA. It should be noted that the partial mineralization of AMX solution (69% TOC removal) obtained in this study is clearly due to relatively low applied current studied (i.e. < 5 mA cm^{-1} current density). A much better mineralization could be achieved at higher current density but may be detrimental to the stability of the anode. However, a new Ti_4O_7 anode that can withstand high current density is currently being developed by our industrial partner (Saint Gobain, France) for application on industrial scale.

A comparison study with other anode materials especially BDD, was made under same experimental conditions (I = 10–120 mA) (Fig. 6b), while experiments were performed at a fixed current of 120 mA for DSA and Pt anodes. As expected, BDD anode shows superior TOC removal compared to Ti_4O_7 anode, especially at high applied current values (i.e. 60 and 120 mA) due to the larger power of BDD for the production of BDD (•OH) from the water oxidation reaction (Eq. (1)). After 480 min of electrolysis, a maximum of 94% TOC removal was achieved at 120 mA with BDD anode compared to 69% obtained at the same current with Ti_4O_7 anode. A much smaller TOC removal of 36% and 41% was obtained with DSA and Pt anode, respectively, demonstrating that these latter anodes have limited mineralization ability for organic pollutants.

Further, increase in applied current from 30 to 60 mA causes a faster TOC decay with BDD (Fig. 6b) compared to Ti_4O_7 anode (Fig. 6a), indicating the high potent of BDD for the production of BDD (•OH) at higher currents. However, increased applied current from 60 to 120 mA shows marginal TOC removal (Fig. 6b) compared to significant increment obtained with Ti_4O_7 anode (Fig. 6a). The decrease in mineralization efficiency observed with BDD anode at higher applied current can be related to the gradual acceleration of parallel non-oxidative reactions consuming hydroxyl radicals, mainly the recombination reactions of BDD (•OH) (Eqs. (6) and (7)) when they are generated at high concentration on the anode surface, in particular, with relatively lower concentrations of organic matter. This was clearly seen in (Fig. 6c and d) where the decay in MCE between 60 and 120 mA was much significant with BDD anode (Fig. 6d) compared to Ti_4O_7 anode (Fig. 6c).

$$2BDD(^{\bullet}OH) \rightarrow 2BDD + O_2(g) + 2H^+ + 2e^- \quad (6)$$

$$2BDD(^{\bullet}OH) \rightarrow 2BDD + H_2O_2 \quad (7)$$

It should be noted that H_2O_2 as an oxidant has minimal contribution to the mineralization of AMX with Ti_4O_7 anode as shown in Fig. 7a, in contrast to oxidation experiments (Fig. 5a). Indeed it can oxidize some easily oxidizable organics but cannot mineralize hardly oxidizable reaction intermediates. Other studies (Sirés et al., 2007, 2010) have shown that *in-situ* generated H_2O_2 has negligible direct effect on the mineralization of organics. In fact, its excessive accumulation may inhibit organic oxidation via the destruction of Ti_4O_7(•OH) in a similar manner to that in Eq. (5), as it was observed in this study after 240 min of electrolysis at 60 mA (Fig. 7a). For instance after 480 min of electrolysis, the mineralization efficiency obtained with and without H_2O_2 generation (carbon-felt and stainless steel cathodes) were 45% and 48% respectively, indicating slight reduction in efficiency with the former.

The stability of the activity of Ti_4O_7anode was also assessed by comparing mineralization experiment after <25 h and >200 h of usage in electrooxidation process at 60 mA. Almost 17% loss in mineralization efficiency was observed after 200 h of utilization (Fig. 7b), with subsequent studies exhibited no significant reduction in mineralization. Such loss in activity of Ti_4O_7 can be explained either by the formation of passivation layer on the surface of the anode or partial conversion of Ti_4O_7 at the surface of the anode to less conducting TiO_2, which can be removed by "soft" sand blasting of the anode surface or polarity inversion to partially restore its activity (Bejan et al., 2009).

3.3. Evolution of the oxidation byproducts of AMX and mineralization pathways

The oxidation of an organic compound containing heteroatoms on a non-active anode such as BDD or Ti_4O_7 usually proceeds via the formation of aromatic by-products, short-chain aliphatic carboxylic acids and inorganic ions. It is important to note that the release of inorganic ions in the electrolyzed solution is a major signal of pollutant mineralization (Lin et al., 2013; Özcan et al., 2008a). Upon covalent bonds cleavage of AMX molecules and oxidation of formed lower molecular weight species, organic N atom was released to the solution and quantified as NH_4^+ and NO_3^- by ion chromatography without detecting NO_2^-, while S atom was recovered as SO_4^{2-} in the treated solutions containing 0.1 mM of AMX (Fig. 8a and b) at 120 mA constant current electrolysis. The

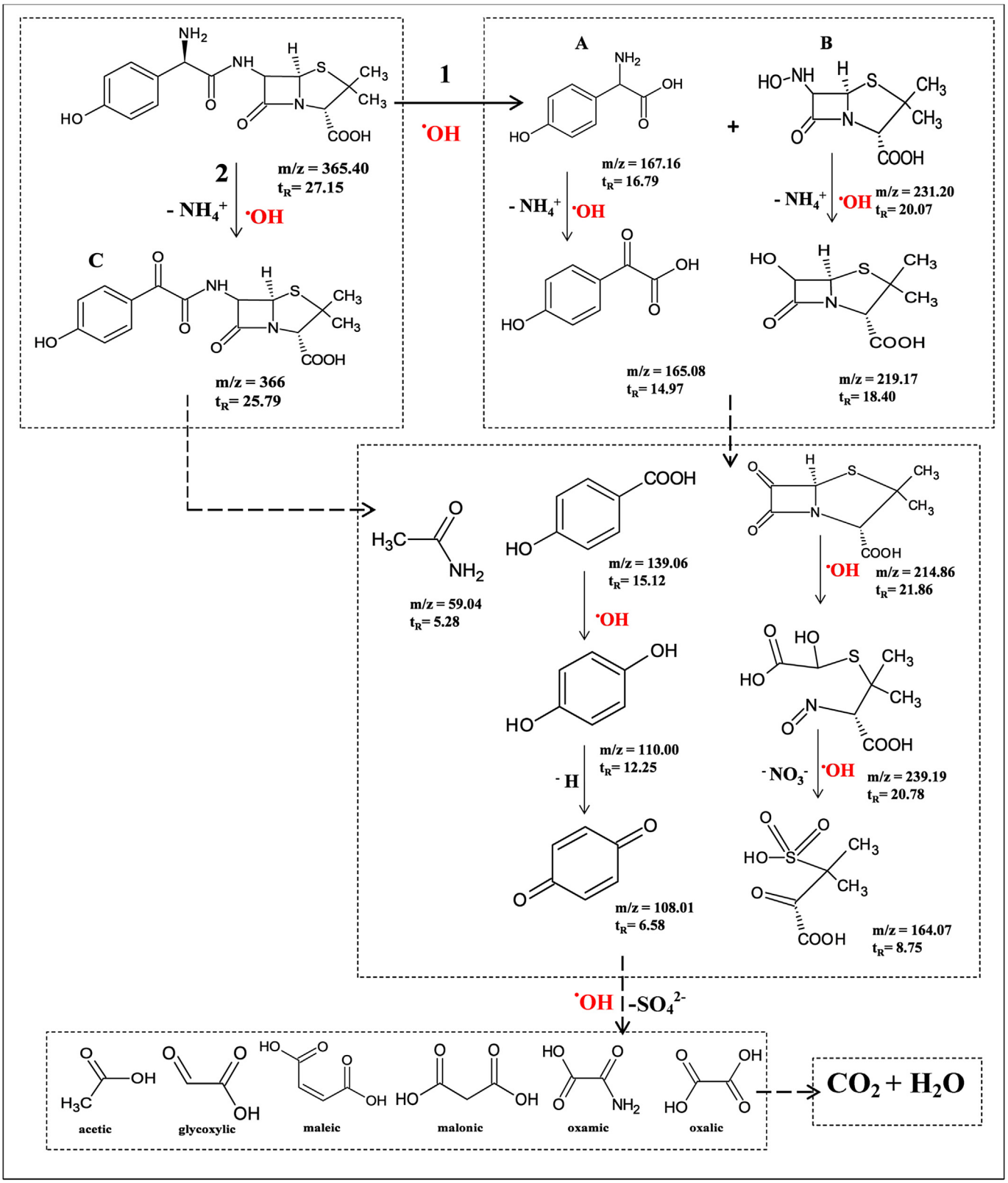

Fig. 10. Proposed reaction mechanism for the total mineralization of AMX by electrooxidation using Ti_4O_7 anode.

amount of both NH_4^+ and NO_3^- ions continuously accumulated in treated solution over 480 min of treatment with either Ti_4O_7 or BDD anode as shown in Fig. 8a and b. Majority of N atom released was detected as NH_4^+, with significant proportion as NO_3^- in both cases, which could be explained by the partial reduction of the small fraction of the formed NO_3^- to NH_4^+ as it has been experimentally confirmed by previous studies (Sirés et al., 2010; Martin de Vidales et al., 2016), although Thiam et al., 2015 did not

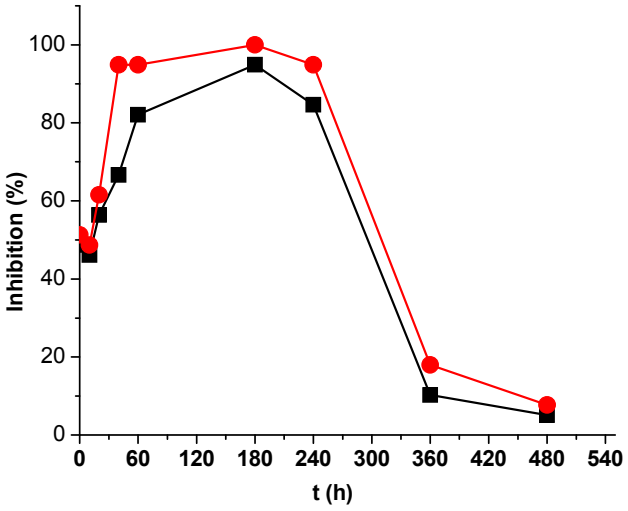

Fig. 11. Toxicity evolution of 0.1 mM AMX solution during electro-oxidation with Ti_4O_7 anode at 120 mA in terms of Inhibition of luminescence of *V. fischeri* bacteria after (-■-) 5 min and (-●-) 15 min exposure time.

observe reduction of NO_3^- to NH4$^+$ on carbon-PTFE air-diffusion cathode. Similarly, S atom is oxidized and gradually accumulated as SO_4^{2-} over the treated time to reach overall 0.1 mM (100% of initial S) with both anodes. After 480 min of electrolysis, 0.141 mM NH_4^+ and 0.068 mM NO_3^- representing 47 and 22% respectively of the initial N atom in 0.1 mM AMX solution (0.3 mM N) was found in the final solution treated with Ti_4O_7 anode, whereas 0.186 mM NH_4^+ (62% of initial N) and 0.086 mM NO_3^- (29% of initial N) was obtained with BDD anode, indicating much better mineralization with BDD anode as shown in Fig. 6b. While the organic S was totally recovered as SO_4^{2-} in the treated solutions, the amount of inorganic N was far less than the total initial N content of 0.1 mM AMX solution (i.e. 69% and 91% for Ti_4O_7 and BDD anodes respectively). In the case of BDD anode, the mass balance is almost complete since the rest of N (9%) is present in oxamic acid that was not mineralized (remained in the solution after treatment) (Fig. 9b). In contrast the mass balance for N is slightly deficient in the case of Ti_4O_7 anode that can be explained by its relatively lower mineralization power (24% of N is present in non-mineralized oxamic acid) (Fig. 9a). The remaining 7% of non-detected N can be present in other non-identified N-containing organics remaining in the treated solution judging from the profiles of NH_4^+, NO_3^- and oxamic acid (Figs. 8a and 9a) which continuously accumulated without sign of reaching plateau after 480 min of treatment or may have been loss as volatile N-compounds (N_xO_y) (Brillas et al., 2010; El-Ghenymy et al., 2013).

Ion-exclusion chromatographs of the treated solution at different electrolysis time showed the formation of several carboxylic acids such as oxalic, oxamic, malonic, maleic, glyoxylic and acetic acids from the cleavage of both aromatics and non-aromatics intermediates by-products. The evolution of these carboxylic acids shown in Fig. 9a and b indicates high accumulation rate at the early stage of electrolyses, with further treatment caused decline in their concentrations especially with BDD anode. In both case, oxalic acid reaches the highest concentration (0.14 mM and 0.08 mM for Ti_4O_7 and BDD anodes respectively) because it is the ultimate product of oxidative cleavage of benzenic moiety of aromatic intermediates (Oturan et al., 2008; Brillas et al., 2010) before mineralization. It must be noted that the persistence of these carboxylic acids after 480 min of electrolysis, specifically with Ti_4O_7 anode accounts for the large residual TOC (Fig. 6a) observed in the treated solution.

To elucidate the mechanism of AMX mineralization during the electrochemical treatment, the intermediates formed after 60 min of electrolysis of 230 mL solution containing 0.3 mM AMX in 0.05 M Na_2SO_4 at 120 mA were identified by GC-MS. Based on the identified intermediate products; two oxidation pathways were proposed (Fig. 10). The first path (**1**) involves the cleavage of the peptide bond closed to phenyl group with the formation of 2-amino (4-hydroxyphenyl) acetic acid (**A**, m/z = 167.16) and a bicyclical lactamic product (**B**, m/z = 231.20), with the latter (**B**) further oxidized in several steps with the release of NH_4^+ and NO_3^- to form an open-chain structure containing sulfonic group. The bicyclical lactamic product (**B**) and its oxidized products observed in this study were also reported for photocatalytic oxidation of AMX (Klauson et al., 2010), which was formed in combination with *p*-hydroxybenzoic acid as a result of N-dealkylation of AMX at the secondary amine group. However in the present studies, *p*-hydroxybenzoic acid (m/z = 139.06) was a product of subsequent hydroxylation and dehydrogenation of **A** at the primary amino group (release as NH_4^+), followed by decarboxylation (elimination of CO_2) reaction. Its further hydroxylation and dehydrogenation forms characteristic intermediate products, hydroquinone (m/z = 110) and benzoquinone (m/z = 108.01), respectively. The second path (**2**) starts with Ti_4O_7(•OH) attack on the primary amino group leading to the formation of product **C** (m/z = 366) which subsequent cleavage at both secondary amine and carbonyl group, forming oxamic acid, acetamide, *p*-hydrobenzoic acid, and a bicyclical lactamic product, that were further oxidized in similar manner to those formed in first path (**1**). The carbonyl intermediates was also reported by Klauson et al., 2010. Further Ti_4O_7(•OH) attack on acetamide, benzoquinone and sulfonic contained structure produces several carboxylic acids such as oxalic, oxamic, malonic, maleic, glyoxylic and acetic acids, that are later oxidized to CO_2, water and inorganic ions (Garcia-Segura and Brillas, 2011).

3.4. Evolution of toxicity of AMX solution during electrooxidation treatment

The change in toxicity of 0.1 mM AMX solution over electrolysis time during electrooxidation treatment with Ti_4O_7 anode at 120 mA was investigated by monitoring the bioluminescence inhibition of *V. fischeri* bacteria caused by the presence of AMX and its oxidation by-products. As depicted in Fig. 11, the bioluminescence inhibition increases at the early stages of electrolysis attaining maximum values of 100%, indicating the formation of aromatic/cyclic organics as the predominant oxidation intermediates which are more toxic than initial AMX molecule. The maximum inhibition persisted up to 240 min of electrolysis due to lower mineralization of these intermediates with Ti_4O_7 anode, which is in agreement with the TOC decay reported in Fig. 6a. A sharp drop in bioluminescence inhibition follows, indicating drastic decay in toxicity owing to the further degradation of the toxic intermediates into less toxic compounds. The bioluminescence inhibition attained its minimum value after 360 min of electrolysis, indicating the mineralization/degradation of both AMX and its oxidation reaction intermediates into less toxic and biodegradable short chain carboxylic acid.

4. Conclusions

From the above results and discussion, we can draw the following main conclusions:

- Ti_4O_7 anode prepared by plasma deposition is an effective anode for electrooxidation of AMX solutions at its natural pH.

- The prepared anode consist only Ti_4O_7 because all the other sub-oxides of TiO_2 formed during the reduction of TiO_2 with coke were transformed to Ti_4O_7 during plasma deposition.
- Faster degradation and relatively high mineralization of AMX have been achieved by electrooxidation with Ti_4O_7 anode compared to DSA and Pt anodes at similar experimental conditions. However it exhibits relatively lower performances compared to BDD anode.
- The decay of AMX always follow pseudo-first order kinetics and the apparent rate constant ($k_{app,\ AMX}$) for oxidation of AMX increased with applied current; enhanced by *in-situ* H_2O_2 generation and diminished with increased initial AMX concentration.
- There is a slight (10%) reduction in the activity of the prepared Ti_4O_7 anode after 200 h of usage, possibly due to passivation.
- The major mineralization end-products after mineralization treatment at 120 mA are short-chain carboxylic and inorganic ions.
- Both aromatic intermediates and bicyclic lactamic products of AMX were identified by GC-MS. Using these data and analysis of released inorganic ions and carboxylic acid, a plausible mineralization pathway of AMX with Ti_4O_7 anode was proposed.
- Initial AMX solution shows relatively high inhibition to *V. fischeri* bacteria, which further increased at the early stage of electrooxidation due to formation of cyclic intermediates but sharply decreased at the later stage of electrolysis.

Since the Ti_4O_7 is produced mainly from TiO_2 which is very cheap and highly abundant material, this anode could be an interesting alternative in industrial wastewater treatment by electrooxidation. Further studies should be performed on its stability in higher applied current conditions and its potential usage as anode in Fenton based EAOPs especially electro-Fenton oxidation, since Fenton based EAOPs usually performed better than corresponding electrooxidation at analogous conditions.

Acknowledgement

The authors thank the EU for providing financial support through the Erasmus Mundus Joint Doctorate Programme ETeCoS^3 (Environmental Technologies for Contaminated Solids, Soils and Sediments, grant agreement FPA n°2010-0009) and the ANR (French National Research Agency)(ANR-13-ECOT-0003-03) funding through ANR EcoTechnologies et EcoServices (ECO TS) of the CElectrON project: “Couplage Electro-Oxydation et Nanofiltration pour le traitement d'effluents”.

References

Ammar, S., Abdelhedi, R., Flox, C., Arias, C., Brillas, E., 2006. Electrochemical degradation of the dye indigo carmine at boron-doped diamond anode for wastewaters remediation. Environ. Chem. Lett. 4, 229–233.
Andersson, S., Collén, B., Kuylenstierna, U., Magnéli, A., Magnéli, A., Pestmalis, H., Åsbrink, S., 1957. Phase analysis studies on the titanium-oxygen system. Acta Chem. Scand. 11, 1641–1652.
Andreozzi, R., Canterino, M., Marotta, R., Paxeus, N., 2005. Antibiotic removal from wastewaters: the ozonation of amoxicillin. J. Hazard. Mater. 122, 243–250.
Bejan, D., Guinea, E., Bunce, N.J., 2012. On the nature of the hydroxyl radicals produced at boron-doped diamond and Ebonex® anodes. Electrochim. Acta 69, 275–281.
Bejan, D., Malcolm, J.D., Morrison, L., Bunce, N.J., 2009. Mechanistic investigation of the conductive ceramic Ebonex® as an anode material. Electrochim. Acta 54, 5548–5556.
Benito-Peña, E., Partal-Rodera, A.I., León-González, M.E., Moreno-Bondi, M.C., 2006. Evaluation of mixed mode solid phase extraction cartridges for the preconcentration of beta-lactam antibiotics in wastewater using liquid chromatography with UV-DAD detection. Anal. Chim. Acta 556, 415–422.
Boye, B., Brillas, E., Marselli, B., Michaud, P.-A., Comninellis, C., Farnia, G., Sandonà, G., 2006. Electrochemical incineration of chloromethylphenoxy herbicides in acid medium by anodic oxidation with boron-doped diamond electrode. Electrochim. Acta 51, 2872–2880.
Brillas, E., Martínez-Huitle, C.A., 2015. Decontamination of wastewaters containing synthetic organic dyes by electrochemical methods. An updated review. Appl. Catal. B Environ. 166–167, 603–643.
Brillas, E., Martínez-Huitle, C.A. (Eds.), 2011. Synthetic Diamond Films: Preparation, Electrochemistry, Characterization, and Applications. John Wiley & Sons, Inc., Hoboken, NJ, USA.
Brillas, E., Garcia-Segura, S., Skoumal, M., Arias, C., 2010. Electrochemical incineration of diclofenac in neutral aqueous medium by anodic oxidation using Pt and boron-doped diamond anodes. Chemosphere 79, 605–612.
Chen, G., 2004. Electrochemical technologies in wastewater treatment. Sep. Purif. Technol. 38, 11–41.
Chen, G., Betterton, E.A., Arnold, R.G., 1999. Electrolytic oxidation of trichloroethylene using a ceramic anode. J. Appl. Electrochem. 29, 961–970.
Ciríaco, L., Anjo, C., Correia, J., Pacheco, M.J., Lopes, A., 2009. Electrochemical degradation of Ibuprofen on Ti/Pt/PbO_2 and Si/BDD electrodes. Electrochim. Acta 54, 1464–1472.
Comninellis, C., 1994. Electrocatalysis in the electrochemical conversion/combustion of organic pollutants for waste water treatment. Electrochim. Acta 39, 1857–1862.
Costanzo, S.D., Murby, J., Bates, J., 2005. Ecosystem response to antibiotics entering the aquatic environment. Mar. Pollut. Bull. 51, 218–223.
Diagne, M., Sharma, V.K., Oturan, N., Oturan, M.A., 2014. Depollution of indigo dye by anodic oxidation and electro-Fenton processes using boron-doped diamond anode. Environ. Chem. Lett. 12, 219–224.
El-Ghenymy, A., Cabot, P.L., Centellas, F., Garrido, J.A., Rodríguez, R.M., Arias, C., Brillas, E., 2013. Electrochemical incineration of the antimicrobial sulfamethazine at a boron-doped diamond anode. Electrochim. Acta 90, 254–264.
Elmolla, E.S., Chaudhuri, M., 2010. Photocatalytic degradation of amoxicillin, ampicillin and cloxacillin antibiotics in aqueous solution using UV/TiO_2 and UV/H_2O_2/TiO_2 photocatalysis. Desalination 252, 46–52.
Elmolla, E.S., Chaudhuri, M., 2009. Degradation of the antibiotics amoxicillin, ampicillin and cloxacillin in aqueous solution by the photo-Fenton process. J. Hazard. Mater. 172, 1476–1481.
Fernandes, A., Pacheco, M.J., Ciríaco, L., Lopes, A., 2012. Anodic oxidation of a biologically treated leachate on a boron-doped diamond anode. J. Hazard. Mater. 199–200, 82–87.
Garcia-Segura, S., Brillas, E., 2011. Mineralization of the recalcitrant oxalic and oxamic acids by electrochemical advanced oxidation processes using a boron-doped diamond anode. Water Res. 45, 2975–2984.
García-Montoya, M.F., Gutiérrez-Granados, S., Alatorre-Ordaz, A., Galindo, R., Ornelas, R., Peralta-Hernández, J.M., 2015. Application of electrochemical/BDD process for the treatment wastewater effluents containing pharmaceutical compounds. J. Ind. Eng. Chem. 31, 238–243.
Geng, P., Su, J., Miles, C., Comninellis, C., Chen, G., 2015. Highly-ordered Magnéli Ti_4O_7 nanotube arrays as effective anodic material for electro-oxidation. Electrochim. Acta 153, 316–324.
Haidar, M., Dirany, A., Sirés, I., Oturan, N., Oturan, M.A., 2013. Electrochemical degradation of the antibiotic sulfachloropyridazine by hydroxyl radicals generated at a BDD anode. Chemosphere 91, 1304–1309.
Heberer, T., 2002. Occurrence, fate, and removal of pharmaceutical residues in the aquatic environment: a review of recent research data. Toxicol. Lett. 131, 5–17.
Javier Benitez, F., Acero, J.L., Real, F.J., Roldán, G., 2009. Ozonation of pharmaceutical compounds: rate constants and elimination in various water matrices. Chemosphere 77, 53–59.
Klauson, D., Babkina, J., Stepanova, K., Krichevskaya, M., Preis, S., 2010. Aqueous photocatalytic oxidation of amoxicillin. Catal. Today 151, 39–45.
Kolbrecka, K., Przyluski, J., 1994. Sub-stoichiometric titanium oxides as ceramic electrodes for oxygen evolution—structural aspects of the voltammetric behaviour of TinO2n−1. Electrochim. Acta 39, 1591–1595.
Kolpin, D.W., Furlong, E.T., Meyer, M.T., Thurman, E.M., Zaugg, S.D., Barber, L.B., Buxton, H.T., 2002. Pharmaceuticals, hormones, and other organic wastewater contaminants in U.S. streams, 1999–2000: a National Reconnaissance. Environ. Sci. Technol. 36, 1202–1211.
Kümmerer, K., 2009. Antibiotics in the aquatic environment – a review – Part I. Chemosphere 75, 417–434.
Lin, H., Niu, J., Xu, J., Li, Y., Pan, Y., 2013. Electrochemical mineralization of sulfamethoxazole by Ti/SnO_2-Sb/Ce-PbO_2 anode: kinetics, reaction pathways, and energy cost evolution. Electrochim. Acta 97, 167–174.
Marselli, B., Garcia-Gomez, J., Michaud, P.-A., Rodrigo, M.A., Comninellis, C., 2003. Electrogeneration of hydroxyl radicals on boron-doped diamond electrodes. J. Electrochem. Soc. 150, D79.
Martin de Vidales, M.J., Millán, M., Sáez, C., Cañizares, P., Rodrigo, M.A., 2016. What happen to the inorganic nitrogen species during conductive diamond electrochemical oxidation of real wastewater? Electrochem. Commun. 67, 65–68.
Martínez-Huitle, C.A., Rodrigo, M.A., Sirés, I., Scialdone, O., 2015. Single and coupled electrochemical processes and reactors for the abatement of organic water pollutants: a critical review. Chem. Rev. 115, 13362–13407.
Martínez-Huitle, C.A., Ferro, S., 2006. Electrochemical oxidation of organic pollutants for the wastewater treatment: direct and indirect processes. Chem. Soc. Rev. 35, 1324.
Muruganathan, M., Yoshihara, S., Rakuma, T., Uehara, N., Shirakashi, T., 2007. Electrochemical degradation of 17β-estradiol (E2) at boron-doped diamond (Si/BDD) thin film electrode. Electrochim. Acta 52, 3242–3249.
Oturan, M.A., Aaron, J.J., 2014. Advanced oxidation processes in water/wastewater

treatment: principles and applications. A review. Crit. Rev. Environ. Sci. Technol. 44, 2577–2641.
Oturan, N., Brillas, E., Oturan, M.A., 2012. Unprecedented total mineralization of atrazine and cyanuric acid by anodic oxidation and electro-Fenton with a boron-doped diamond anode. Environ. Chem. Lett. 10, 165–170.
Oturan, M.A., Pimentel, M., Oturan, N., Sirés, I., 2008. Reaction sequence for the mineralization of short-chain carboxylic acids usually formed upon cleavage of aromatics during electrochemical Fenton treatment. Electrochim. Acta 54, 173–182.
Özcan, A., Şahin, Y., Koparal, A.S., Oturan, M.A., 2008a. Propham mineralization in aqueous medium by anodic oxidation using boron-doped diamond anode: influence of experimental parameters on degradation kinetics and mineralization efficiency. Water Res. 42, 2889–2898.
Özcan, A., Şahin, Y., Savaş Koparal, A., Oturan, M.A., 2008b. Carbon sponge as a new cathode material for the electro-Fenton process: comparison with carbon felt cathode and application to degradation of synthetic dye basic blue 3 in aqueous medium. J. Electroanal. Chem. 616, 71–78.
Panizza, M., Cerisola, G., 2009. Direct and mediated anodic oxidation of organic pollutants. Chem. Rev. 109, 6541–6569.
Panizza, M., Cerisola, G., 2005. Application of diamond electrodes to electrochemical processes. Electrochim. Acta 51, 191–199.
Panizza, M., Dirany, A., Sirés, I., Haidar, M., Oturan, N., Oturan, M.A., 2014. Complete mineralization of the antibiotic amoxicillin by electro-Fenton with a BDD anode. J. Appl. Electrochem 44, 1327–1335.
Pignatello, J.J., Oliveros, E., MacKay, A., 2006. Advanced oxidation processes for organic contaminant destruction based on the Fenton reaction and related chemistry. Crit. Rev. Environ. Sci. Technol. 36, 1–84.
Pruden, A., 2014. Balancing water sustainability and public health goals in the face of growing concerns about antibiotic resistance. Environ. Sci. Technol. 48, 5–14.
Rodrigo, M.A., Oturan, N., Oturan, M.A., 2014. Electrochemically assisted remediation of pesticides in soils and water: a review. Chem. Rev. 114, 8720–8745.
Rodrigo, M.A., Cañizares, P., Sánchez-Carretero, A., Sáez, C., 2010. Use of conductive-diamond electrochemical oxidation for wastewater treatment. Catal. Today 151, 173–177.
Santos, D., Pacheco, M.J., Gomes, A., Lopes, A., Ciríaco, L., 2013. Preparation of Ti/Pt/SnO_2–Sb_2O_4 electrodes for anodic oxidation of pharmaceutical drugs. J. Appl. Electrochem. 43, 407–416.
Sirés, I., Brillas, E., Oturan, M.A., Rodrigo, M.A., Panizza, M., 2014. Electrochemical advanced oxidation processes: today and tomorrow: a review. Environ. Sci. Pollut. Res. 2 (1), 8336–8367.
Sirés, I., Oturan, N., Oturan, M.A., 2010. Electrochemical degradation of β-blockers. Studies on single and multicomponent synthetic aqueous solutions. Water Res. 44, 3109–3120.
Sirés, I., Oturan, N., Oturan, M.A., Rodríguez, R.M., Garrido, J.A., Brillas, E., 2007. Electro-Fenton degradation of antimicrobials triclosan and triclocarban. Electrochim. Acta 52, 5493–5503.
Smith, J.R., Walsh, F.C., Clarke, R.L., 1998. Electrodes based on Magneli phase titanium oxides: the properties and applications of Ebonex$^{(R)}$ materials. J. Appl. Electrochem. 28, 1021–1033.
Solano, A.M.S., Araujo, C.K.C., de Melo, J.V., Peralta-Hernandez, J.M., da Silva, D.R., Martinez-Huitle, C.A., 2013. Decontamination of real textile industrial effluent by strong oxidant species electrogenerated on diamond electrode: viability and disadvantages of this electrochemical technology. Appl. Catal. B Environ. 130–131, 112–120.
Sopaj, F., Rodrigo, M.A., Oturan, N., Podvorica, F.I., Pinson, J., Oturan, M.A., 2015. Influence of the anode materials on the electrochemical oxidation efficiency. Application to oxidative degradation of the pharmaceutical amoxicillin. Chem. Eng. J. 262, 286–294.
Thiam, A., Brillas, E., Centellas, F., Cabot, P.L., Sirés, I., 2015. Electrochemical reactivity of Ponceau 4R (food additive E124) in different electrolytes and batch cells. Electrochim. Acta 173, 523–533.
Trovó, A.G., Pupo Nogueira, R.F., Agüera, A., Fernandez-Alba, A.R., Malato, S., 2011. Degradation of the antibiotic amoxicillin by photo-Fenton process – chemical and toxicological assessment. Water Res. 45, 1394–1402.
Walsh, F.C., Wills, R.G.A., 2010. The continuing development of Magnéli phase titanium sub-oxides and Ebonex® electrodes. Electrochim. Acta 55, 6342–6351.
Yu, X., Zhou, M., Hu, Y., Groenen Serrano, K., Yu, F., 2014. Recent updates on electrochemical degradation of bio-refractory organic pollutants using BDD anode: a mini review. Environ. Sci. Pollut. Res. 21, 8417–8431.
Zaky, A.M., Chaplin, B.P., 2014. Mechanism of p-substituted phenol oxidation at a Ti_4O_7 reactive electrochemical membrane. Environ. Sci. Technol. 48, 5857–5867.
Zaky, A.M., Chaplin, B.P., 2013. Porous substoichiometric TiO_2 anodes as reactive electrochemical membranes for water treatment. Environ. Sci. Technol. 47, 6554–6563.
Zhou, M., Liu, L., Jiao, Y., Wang, Q., Tan, Q., 2011. Treatment of high-salinity reverse osmosis concentrate by electrochemical oxidation on BDD and DSA electrodes. Desalination 277, 201–206.